

Chapter 4

Absorbing Boundary Conditions and Waveguide Discontinuities

4.1 Absorbing Boundary Conditions

To analyze planar waveguide structures numerically, they must be enclosed by walls to limit the area of discretization. The use of electrical or magnetic walls produces errors, since the corresponding tangential field components, E_y and H_y , are set to zero. This electric/magnetic wall reflects back the radiated waves into the problem space producing errors in the computed results. To overcome this difficulty, free space can be simulated at an arbitrarily fixed position by using a numerical absorbing boundary conditions (ABC) [60].

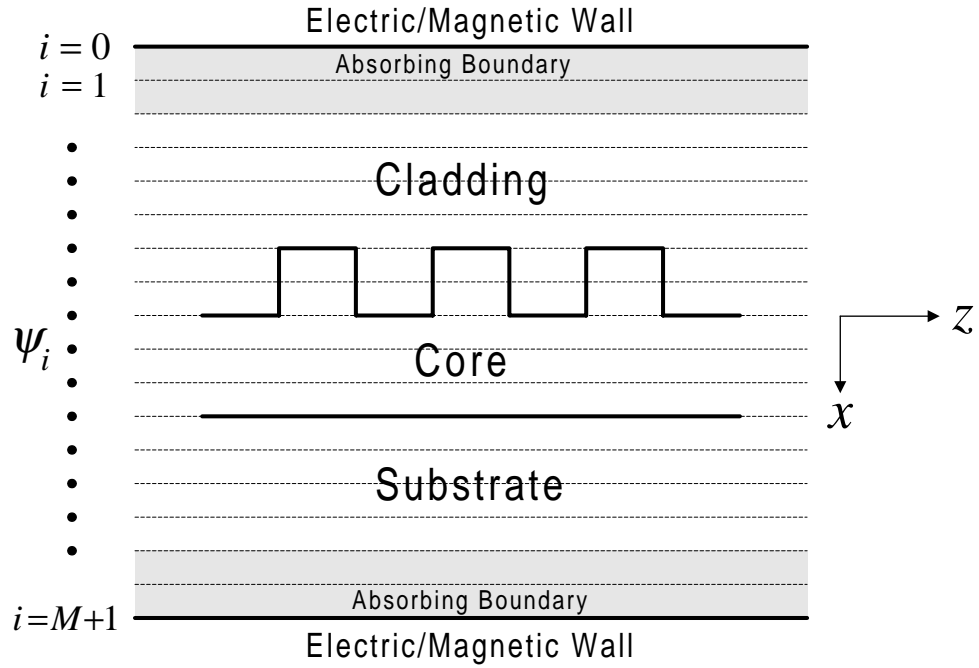


Figure 4.1: Mesh Discretization in the MOL with Absorbing Boundary

4.2 Perfectly Matched Layer

The perfectly matched layer (PML) as a material absorbing boundary condition is introduced for electromagnetic waves by Berenger [61]. This material absorbing boundary condition is based on a non-Maxwellian approach and has been applied to a variety of time-domain problems. A PML absorbing scheme based on complex distance approach was first incorporated into the MOL by Al-Bader and Al-Jamid [37]. This approach was shown to be equivalent to Berenger's method. This type of PML which provides reflectionless absorption at a wide range of incident angles and frequencies [37] independent of polarization, makes it particularly suited for truncating the computational window in the MOL calculations. The absorption of the radiative wave is done by changing the distance x from real to complex. This

introduces an numerical attenuation factor in the radiative field and hence causes decay of the radiative field in the PML region. The last mesh point is terminated by an electric/magnetic wall boundary condition. In this approach the real distance is transformed to a complex one according to:

$$x \rightarrow x(1 + j\sigma) \quad (4.1)$$

where σ is the decay factor constant. The wave radiative e^{+jkx} propagating in $+x$ direction in the real space will be converted to

$$e^{+jkx(1+j\sigma)} = e^{+jkx} e^{-k\sigma x} \quad (4.2)$$

in the complex space. The factor $e^{-k\sigma x}$ causes the decay of the field in the $+x$ direction. The value of σ is set arbitrarily and the number of samples in the PML absorber is chosen to cause a significant decay in the field so that it becomes negligible at the electric/magnetic wall. The choice of the decay factor σ is discussed in reference [62]. If the PML region is made sufficiently wide, only negligible reflections at the extreme edges of the computational window may occur. However, significant numerical reflection may occur at the inner wall of the PML [63]. The choice of σ and the number of sample points in the PML are chosen appropriately in order to minimize reflection from the inner wall of the PML. This PML absorbing scheme is incorporated into the MOL and used throughout this thesis.

Gaussian Field Propagation in Air:

The performance of PML is analyzed by modeling free-space surrounded by PML layers on both sides. A Gaussian field is launched in air and its propagation along the z direction is observed (see figures 4.3-4.10). An analytical expression based

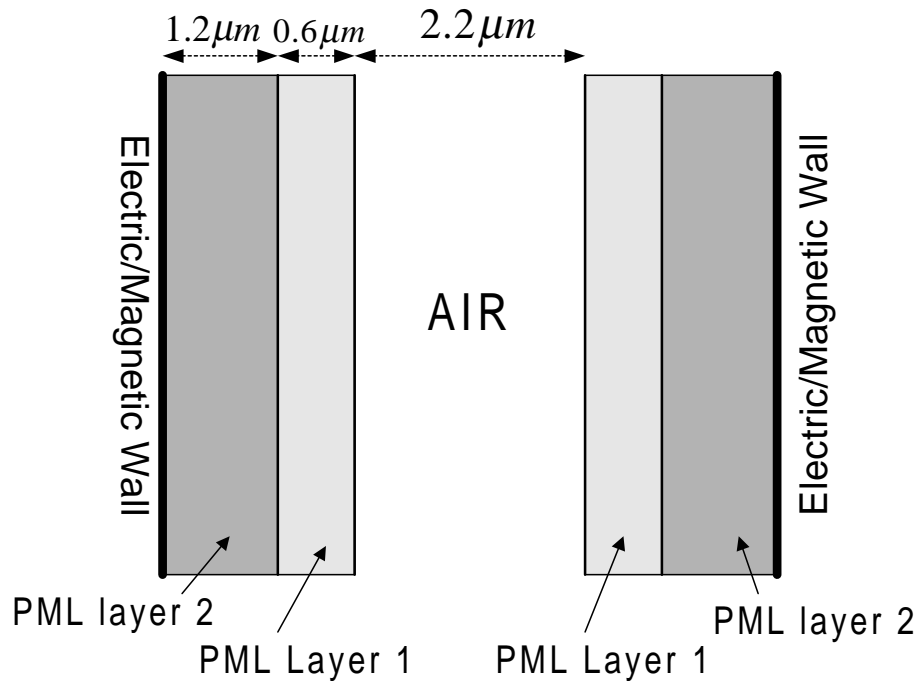


Figure 4.2: A Perfectly Matched Layer (PML) Scheme

on scalar diffraction theory is used to calculate the spread of Gaussian field [59] as it propagates in a medium. The MOL propagated field is compared against the analytically propagated field over a large distance. Each PML layer has 5 sample points with $\sigma = 1$. A non-uniform double layer scheme is used to model a relatively thicker PML. Thus, the field magnitude at the last mesh point drops considerably

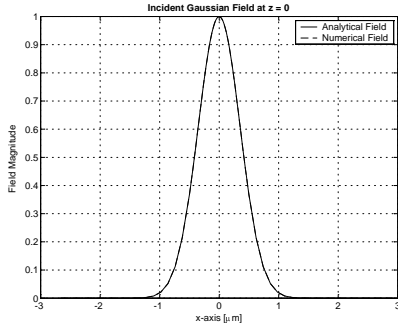


Figure 4.3: Incident Gaussian Field

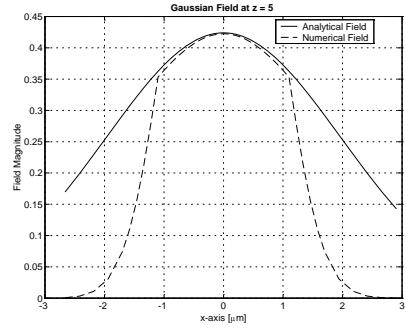


Figure 4.4: Field at $z = 5\mu\text{m}$

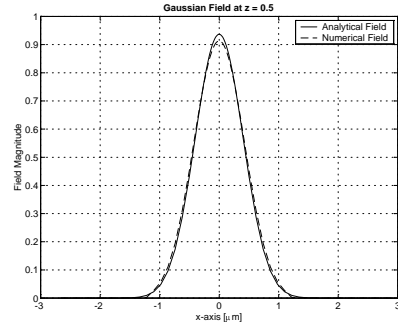


Figure 4.5: Field at $z = 0.5\mu\text{m}$

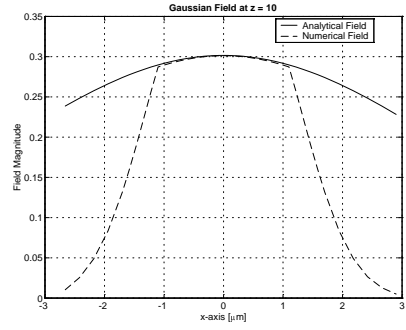


Figure 4.6: Field at $z = 10\mu\text{m}$

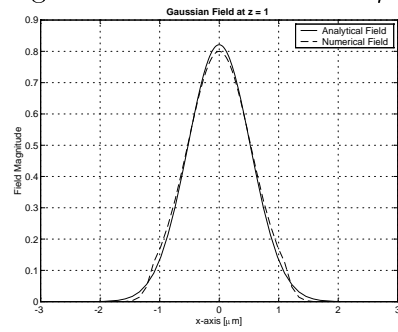


Figure 4.7: Field at $z = 1\mu\text{m}$

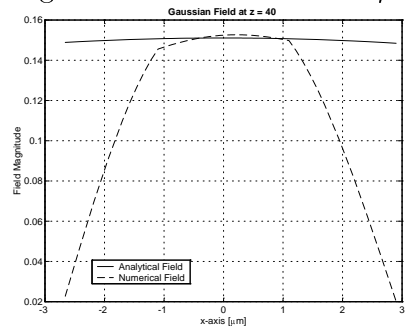


Figure 4.8: Field at $z = 40\mu\text{m}$

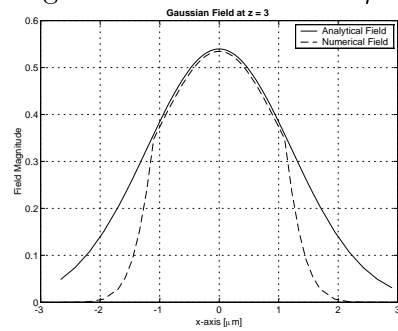


Figure 4.9: Field at $z = 3\mu\text{m}$

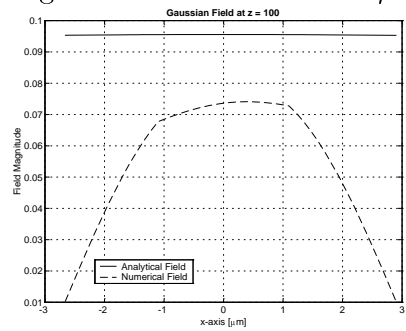


Figure 4.10: Field at $z = 100\mu\text{m}$

due to the $e^{-k\sigma x}$ factor appearing in equation 4.2. The problem space is finally terminated by an electric/magnetic wall. The visual comparison of the analytical field and the MOL computed field shows that the two fields are almost identical over a long propagation distance. This shows the PML absorbs radiative fields and correctly models open-space.

4.3 Waveguide Discontinuities

Discontinuity problems are important in the investigation of optical devices, such as laser facets, gratings, waveguide ends, and connections of different waveguide sections. The classic problem to model scattering from a single and multiple discontinuities has been solved by many workers using different analytical and numerical methods such as the Mode Matching Method [28], the Method of Lines [44, 46, 47, 64] and the Equivalent Transmission-Line Network Method [65]. A good reference to these methods is given in references [28] and [66]. The MOL has been applied to solve a variety of scattering problems, including non-linear scattering problem from a single discontinuity [67] and surface-plasmon mode scattering [68, 69].

4.4 Single Discontinuity

Consider a waveguide having a single discontinuity as shown in figure 4.11. The problem space is divided into two regions, region 0 and region 1. The field is incident

from region 0 resulting in a reflected field in region 0 and a transmitted field in region 1. The total field in each region is the sum of the forward traveling field, e^{+jS_0z} , and the backward traveling field, e^{-jS_0z} .

The total field (Ψ_0) in region 0 is the sum of the incident and reflected fields:

$$\Psi_0 = e^{+jS_0z} A_0 + e^{-jS_0z} B_0 \quad (4.3)$$

The total field (Ψ_1) in region 1 is only the transmitted field:

$$\Psi_1 = e^{+jS_1z} A_1 \quad (4.4)$$

where Ψ is a column vector containing the sampled fields. A_0 , B_0 and A_1 are constant vectors, $S = \sqrt{Q}$ and Q is defined in chapter 3. For TM polarization, Ψ is continuous at the interface at $z = 0$, that is $\Psi_0|_{z=0} = \Psi_1|_{z=0}$. From equations 4.3 and 4.4, we have:

$$A_0 + B_0 = A_1 \quad (4.5)$$

From the interface condition equation 3.27, the field on either side of the discontinuity at $z = 0$ is related by:

$$\Psi'_0 = \frac{N_0}{N_1} \Psi'_1 \quad (4.6)$$

$$(N_0)^{-1} \Psi'_0 = (N_1)^{-1} \Psi'_1 \quad (4.7)$$

where the matrix N is a diagonal matrix of refractive index squared n_i^2 at each sample point. Differentiating equation 4.3 with respect to z and evaluating the result at the interface $z = 0$, we have:

$$\Psi'_0 = jS_0 e^{jS_0z} A_0 - jS_0 e^{-jS_0z} B_0 \quad (4.8)$$

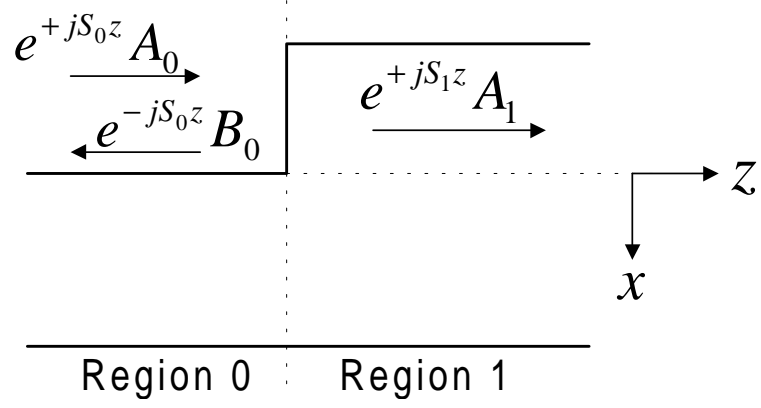


Figure 4.11: A Single Waveguide Discontinuity

$$\Psi'_0|_{z=0} = jS_0(A_0 - B_0) \quad (4.9)$$

Similarly from equation 4.4, we have:

$$\Psi'_1 = jS_1 e^{jS_1 z} A_1 \quad (4.10)$$

$$\Psi'_1|_{z=0} = jS_1 A_1 \quad (4.11)$$

Substituting equations 4.9 and 4.11 into equation 4.7 and simplifying we have:

$$(N_0)^{-1} S_0 (A_0 - B_0) = (N_1)^{-1} S_1 A_1 \quad (4.12)$$

$$(A_0 - B_0) = S_0^{-1} (N_0) (N_1)^{-1} S_1 A_1 \quad (4.13)$$

Eliminating B_0 from equations 4.5 and 4.13, we get the transmitted field, A_1 :

$$A_1 = 2(I + S_0^{-1} N_0 N_1^{-1} S_1)^{-1} A_0 \quad (4.14)$$

$$A_1 = T A_0 \quad (4.15)$$

where T is the transmission matrix. Similarly eliminating A_0 , we get the reflected field, B_0 :

$$B_0 = (I - S_0^{-1} N_0 N_1^{-1} S_1) (I + S_0^{-1} N_0 N_1^{-1} S_1)^{-1} A_0 \quad (4.16)$$

$$B_0 = RA_0 \quad (4.17)$$

where R is the reflection matrix.

For the TE polarization, both field and its z derivatives are continuous across the interface. We follow the same procedure to derive the transmission (T) and reflection (R) matrices for the TE case.

$$A_1 = 2(I + S_0^{-1}S_1)^{-1}A_0 = TA_0 \quad (4.18)$$

$$B_0 = (I - S_0^{-1}S_1)(I + S_0^{-1}S_1)^{-1}A_0 = RA_0 \quad (4.19)$$

The transmission matrix T and the reflection matrix R are related by:

$$A_1 = B_0 + A_0 \quad (4.20)$$

$$= RA_0 + A_0 \quad (4.21)$$

$$= (R + I)A_0 = TA_0 \quad (4.22)$$

4.4.1 Results

A single waveguide discontinuity is modeled as shown in figure 4.12 at $\lambda = 0.86 \mu m$. The TM_0 mode of the narrow waveguide is incident from the left on the waveguide. The reflected and transmitted fields are calculated and propagated backward and forward in the respective waveguides. The problem space is terminated with a single layer PML on both sides. The results are shown in figures 4.13 and 4.14. The reflected field consists of the TM_0 mode of the narrow waveguide after propagating backward a long distance as the radiative part of the field leaks out and absorbed by the PML layers. This shows that the PML absorbs the radiative fields effectively.

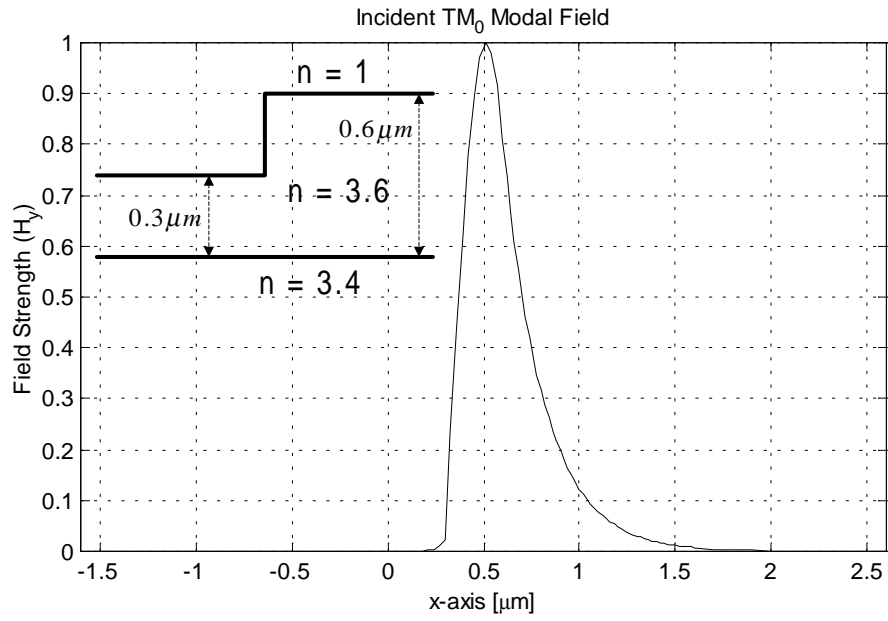


Figure 4.12: Incident TM_0 Modal Field at the Discontinuity

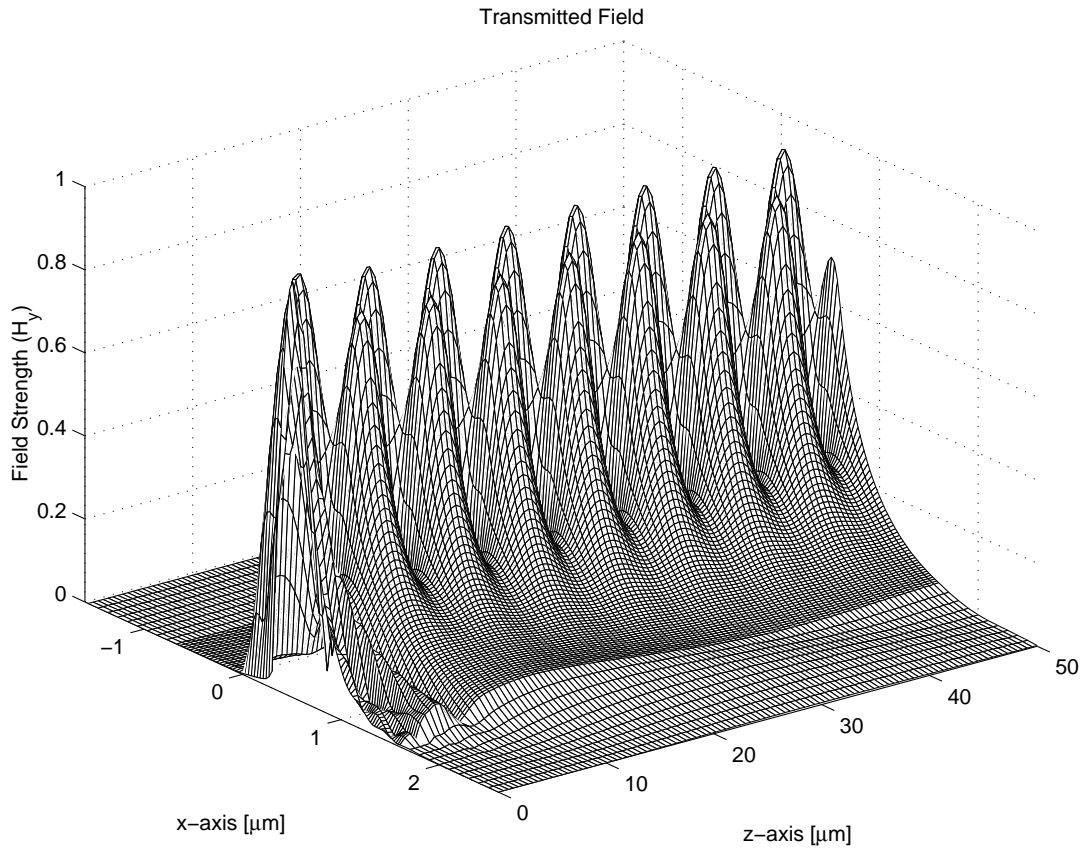


Figure 4.13: Transmitted Field

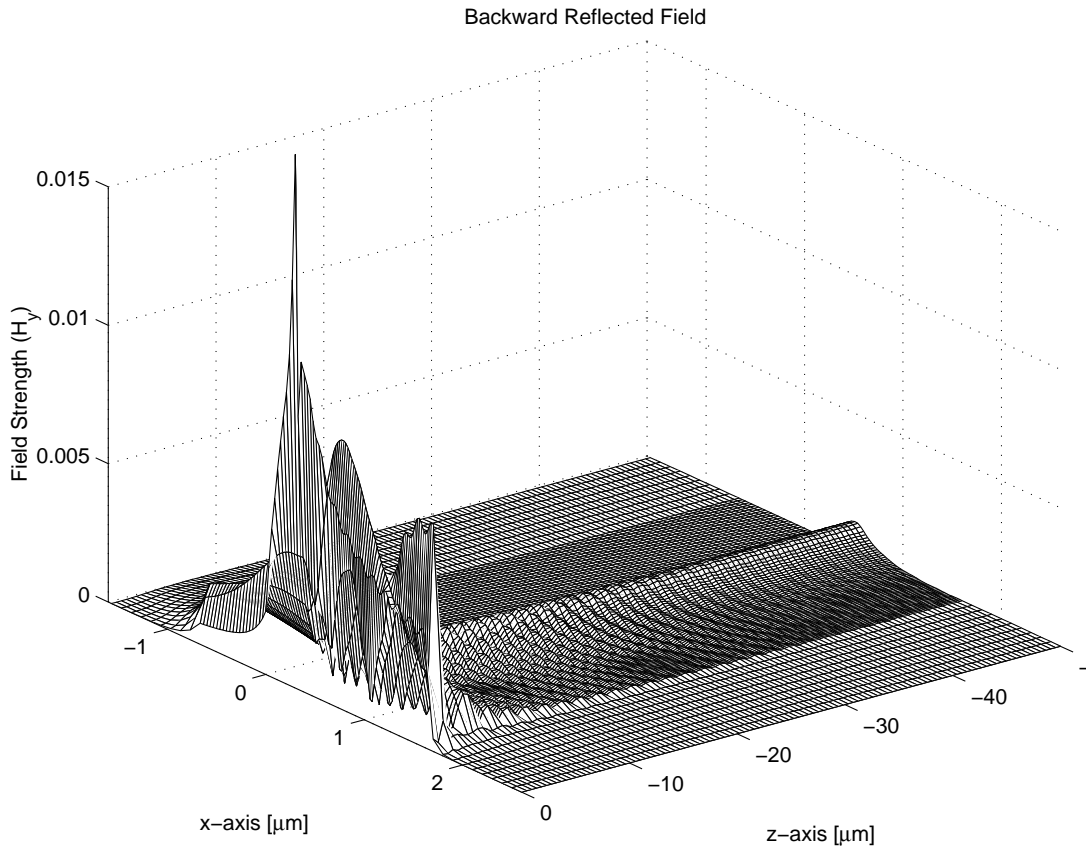


Figure 4.14: Backward Reflected Field

4.5 Double Discontinuity

Consider a waveguide having a double discontinuity as shown in figure 4.15. The problem space is divided into three regions, region 0, region 1 and region 2. The total field in each region is the sum of the forward traveling field, e^{+jS_z} , and the backward traveling field, e^{-jS_z} .

The field is incident from region 0. After reflection from the first discontinuity at $z = 0$, there is a reflected field in region 0 and a transmitted field in region 1. The transmitted field in region 1 is the incident at the second discontinuity $z = d$,

thus there is a reflected field in region 1 and a transmitted field in region 2.

Thus the total field in all three regions is given by:

$$\Psi_0 = e^{+jS_0z}A_0 + e^{-jS_0z}B_0 \quad (4.23)$$

$$\Psi_1 = e^{+jS_1z}A_1 + e^{-jS_1(z-d)}B_1 \quad (4.24)$$

$$\Psi_2 = e^{+jS_2(z-d)}A_2 \quad (4.25)$$

For the TE polarization, the field vector Ψ and its derivative Ψ' with respect to z are continuous at a discontinuity. Applying the interface condition $\Psi_0|_{z=0} = \Psi_1|_{z=0}$, we get:

$$A_0 + B_0 = A_1 + e^{+jS_1d}B_1 \quad (4.26)$$

Similarly applying the interface condition $\Psi'_0|_{z=0} = \Psi'_1|_{z=0}$, we get:

$$S_0A_0 - S_0B_0 = S_1A_1 - S_1e^{+jS_1d}B_1 \quad (4.27)$$

$$T_1(A_0 - B_0) = A_1 - e^{+jS_1d}B_1 \quad (4.28)$$

where $T_1 = S_1^{-1}S_0$. Similarly applying the interface conditions at $z = d$ and simplifying, we get:

$$e^{+jS_1d}A_1 + B_1 = A_2 \quad (4.29)$$

$$T_2(e^{+jS_1d}A_1 - B_1) = A_2 \quad (4.30)$$

where $T_2 = S_2^{-1}S_1$. By eliminating A_1 and B_1 from equations 4.26, 4.28, 4.29 and 4.30, we get the total transmitted and reflected fields [36]:

$$A_2 = (I + T_2)^{-1}T_2e^{+jS_1d}K_4A_0 \quad (4.31)$$

$$B_0 = K_3A_0 \quad (4.32)$$

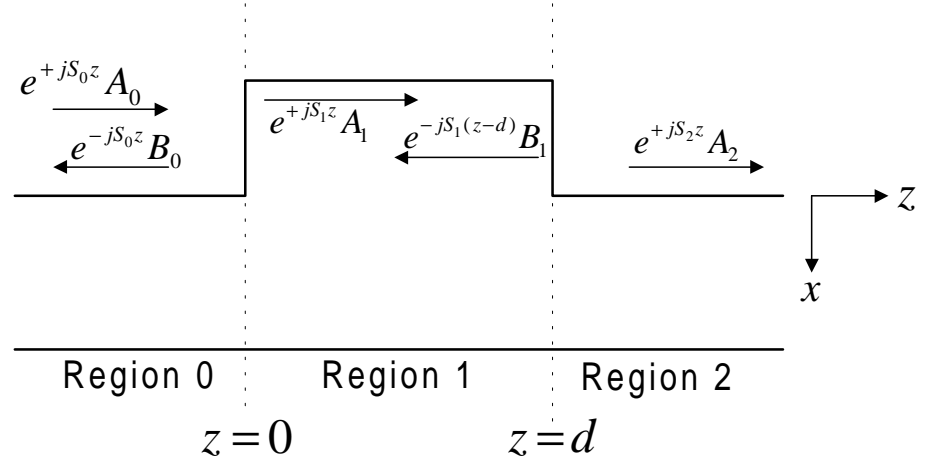


Figure 4.15: A Double Waveguide Discontinuity

where

$$K_4 = (I + T_1) + (I - T_1)K_3 \quad (4.33)$$

and

$$K_3 = (S_1 + S_2)^{-1}(S_2 - S_1) \quad (4.34)$$

For the TM polarization, the results are similar but with $T_1 = S_1^{-1}N_1N_0^{-1}S_0$ and $T_2 = S_2^{-1}N_2N_1^{-1}S_1$.

4.5.1 Results

A double waveguide discontinuity (see figure 4.16) is modeled at $\lambda = 0.86 \mu m$. The TM_0 mode of the narrow waveguide is incident from the left on the junction. The reflected and transmitted fields are calculated and propagated backward and forward in the respective waveguides. The results are shown in figures 4.17 and

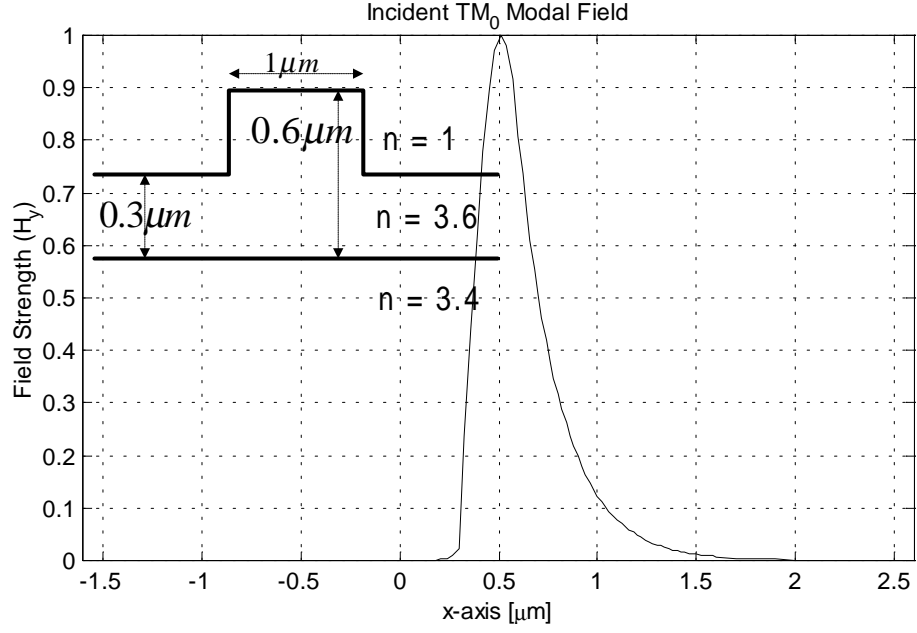


Figure 4.16: Incident TM_0 Modal Field at the First Discontinuity

4.18. The reflected field develops to the TM_0 mode of the narrow waveguide after propagating backward a long distance as the radiative energy leaks out. Similarly, the transmitted field gradually develops into the TM_0 mode of the narrow output waveguide.

4.6 Multiple Discontinuities

Consider the multi-layer structure shown in figure 4.19 [49]. The total field is composed of forward traveling field and backward traveling field. Thus, the total field in each layer is expressed as:

$$\Psi_0 = e^{+jS_0z} A_0 + e^{-jS_0z} B_0 \quad (4.35)$$

$$\Psi_1 = e^{+jS_1z} A_1 + e^{-jS_1(z-d_1)} B_1 \quad (4.36)$$

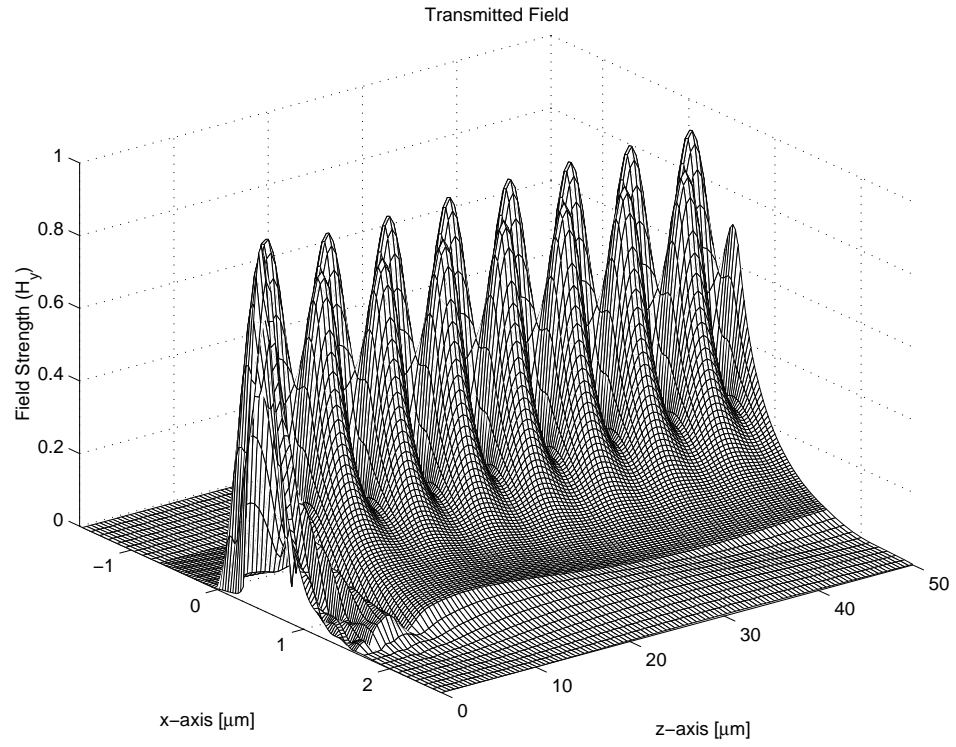


Figure 4.17: Transmitted Field after the Second Discontinuity

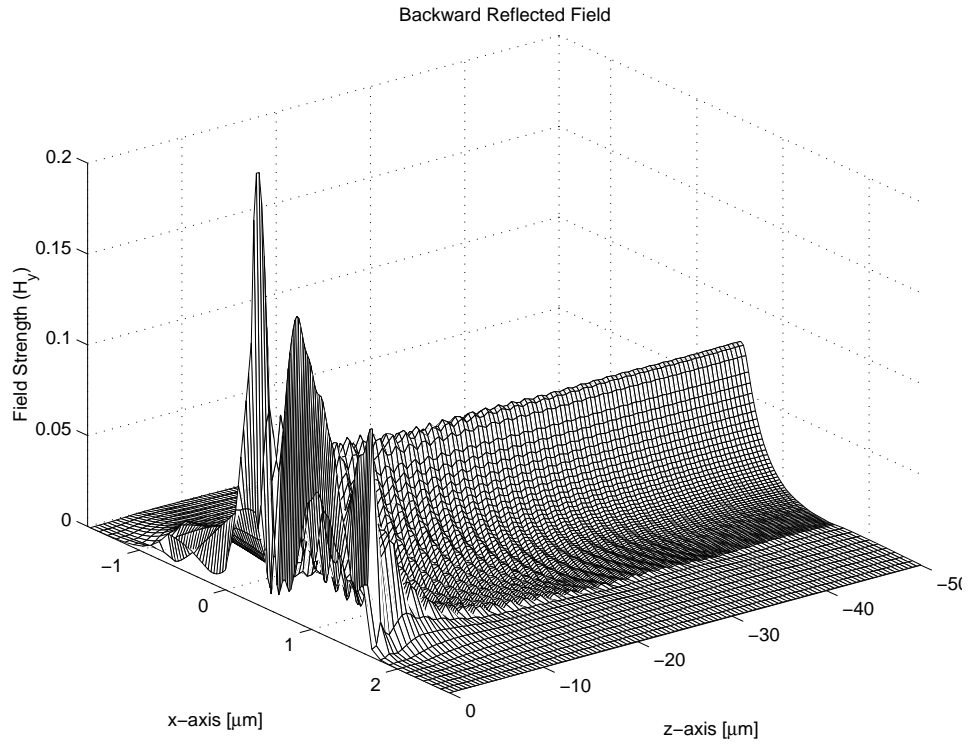


Figure 4.18: Backward Reflected Field from the First Discontinuity

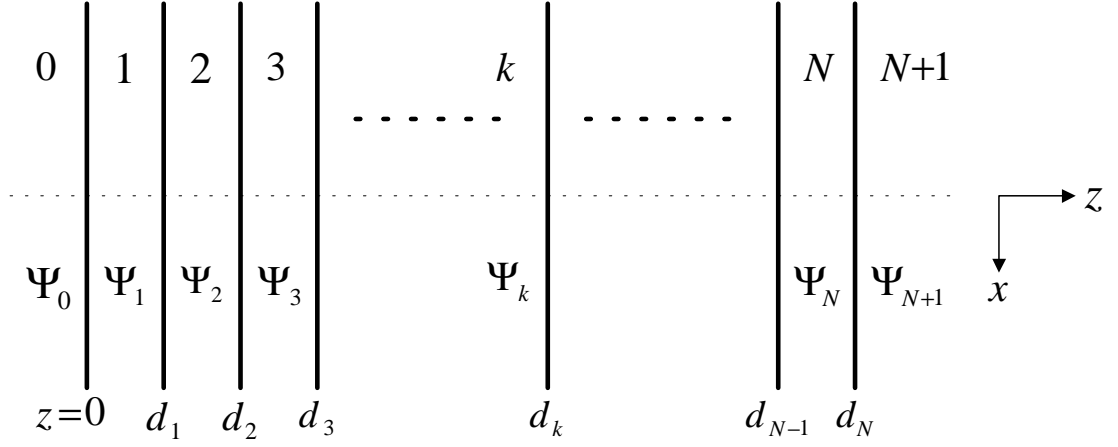


Figure 4.19: Multiple Waveguide Discontinuities

$$\begin{aligned} & \vdots \\ \Psi_k &= e^{+jS_k(z-d_{k-1})}A_k + e^{-jS_k(z-d_k)}B_k \end{aligned} \quad (4.37)$$

$$\begin{aligned} & \vdots \\ \Psi_{N+1} &= e^{+jS_{N+1}(z-d_N)}A_{N+1} \end{aligned} \quad (4.38)$$

The subscript k in Ψ_k and S_k denotes that the column vector Ψ_k and the matrix S_k in the k region. In figure 4.19, the wave is incident on the interface $z = 0$ from the left. In region $N + 1$, the wave is assumed to propagate without reflection in the $+z$ direction. At each discontinuity, the boundary condition requires the continuity of the tangential fields, E_y and H_x . In other words, the continuity of Ψ and $\frac{d\Psi}{dz}$ must be satisfied at the interfaces. Application of these conditions results in the following relationships [49]:

$$e^{jS_k(d_k-d_{k-1})}A_k = \frac{1}{2}(I + S_k^{-1}S_{k+1})A_{k+1} + \frac{1}{2}(I - S_k^{-1}S_{k+1})e^{jS_{k+1}(d_{k+1}-d_k)}B_{k+1} \quad (4.39)$$

$$B_k = \frac{1}{2}(I - S_k^{-1}S_{k+1})A_{k+1} + \frac{1}{2}(I + S_k^{-1}S_{k+1})e^{jS_{k+1}(d_{k+1}-d_k)}B_{k+1} \quad (4.40)$$

where $k = 0, 1, 2, \dots, N$, For $k = 0$, $d_0 = d_{-1} = 0$ and for $k = N$, $B_{N+1} = 0$.

This is a recursive relationship which expresses the field in layer k in terms of the field in layer $k + 1$. We start from the last layer, in which there is only a forward propagating wave, and work backward layer by layer, until we reach the first layer. Thus the field in last layer is expressed in terms of the field in first layer. From this, we can find the reflection and transmission matrices and hence the reflected and transmitted fields. The field in the intermediate layers can also be calculated if required.